Accepted Manuscript

A QTAIM Exploration of the Competition Between Hydrogen and Halogen Bonding in halogenated 1-methyluracil: Water systems

Guo Huan, Tianlv Xu, Roya Momen, Lingling Wang, Yang Ping, Steven R. Kirk, Samantha Jenkins, Tanja van Mourik

Please cite this article as: G. Huan, T. Xu, R. Momen, L. Wang, Y. Ping, S.R. Kirk, S. Jenkins, T. van Mourik, A QTAIM Exploration of the Competition Between Hydrogen and Halogen Bonding in halogenated 1-methyluracil: Water systems, *Chemical Physics Letters* (2016), doi: http://dx.doi.org/10.1016/j.cplett.2016.09.031

A QTAIM Exploration of the Competition Between Hydrogen and Halogen Bonding in halogenated 1-methyluracil:water systems

Guo Huan[a], Tianlv Xu[a], Roya Momen[a], Lingling Wang[a], Yang Ping[a], Steven R. Kirk[a*], Samantha Jenkins[a**]

and Tanja van Mourik[b]

[*]*e-mail: steven.kirk@cantab.net*
[**]*e-mail: samanthajsuman@gmail.com*

[a]*Key Laboratory of Chemical Biology and Traditional Chinese Medicine Research and Key Laboratory of Resource Fine-Processing and Advanced Materials of Hunan Province of MOE, College of Chemistry and Chemical Engineering, Hunan Normal University, Changsha Hunan 410081, China.*
[b]*EaStCHEM School of Chemistry, University of St Andrews, North Haugh, St Andrews, Fife KY16 9ST, Scotland, United Kingdom.*

Using QTAIM we show that the hydrogen bonding complexes of 5-halogenated-1-methyluracil (XmU; X = F, Cl, Br, I or At) with a water molecule were always stronger than the corresponding halogen bonds. The strength of the hydrogen bond decreased with increasing halogen size. The hydrogen bonds displayed an admixture of covalent character but all the halogen bonds were purely electrostatic in nature. An F---O halogen bond was found and was facilitated by an intermediate F---H bonding interaction. The metallicity $\xi(\mathbf{r}_b)$ of the C=O bonds neighboring the hydrogen bonds and of the C-X bonds contiguous with the halogen bonds was explored.

The hydrogen bond and the halogen bond represent two categories of important noncovalent interactions that play prominent roles in experimental and theoretical fields[1-4]. Hydrogen bond and halogen bond interactions were initially referred to as "electron donor-acceptor" or "charge transfer" interactions[5,6].

Among the various intermolecular interactions hydrogen and halogen bonds[7,8] are central to biological molecular systems[9,10] and in atomic excitation and ionization phenomena[11]. The directionality is a critical property in making hydrogen bonds and halogen bonds so useful in some fields[12,13]. There are two key properties that distinguish halogen bonds from hydrogen bonds. The first difference is that for hydrogen bond, the hydrogen atom is shared between an atom, group or molecule that 'donates and another that 'accepts' it[14]. The second difference is that properties of halogens such as the atom size are significantly different compared with those of hydrogen[15]. Similarities and differences of the fundamental intrinsic properties of halogen and hydrogen bonds have been extensively studied theoretically[16]. Previously, various properties of halogen/hydrogen bonds have been studied including molecular electrostatic potential, bond distance, size and polarizability[14,17].

Previous energetics studies noted that the nuclear geometries explain the observation that electrophiles tend to approach the halogen in the C---Y halogen bond, where Y = Cl, Br or I, in a side-on manner nearly perpendicular to the C---Y bond, whereas nucleophiles approach head-on[18,19]. The electron deficiency at the end of the halogens, labeled a σ-hole, was attributed as the reason for the observed strong directionality of halogen bonds, with halogen bond angles typically between 160°-180°.

Fluorine is not generally considered to form halogen bonds, explained by the high electronegativity of fluorine and its tendency to engage in significant sp hybridization producing an influx of negative charge into the region where the positive σ-hole would be[7,8]. There is controversy as to whether organic fluorines can form halogen bonds when strongly electronegative substituents are bound to the carbon[9,10,20] due to fundamental differences between these interactions and halogen bonds involving Cl, Br and I[15]. Halogen bonding strength is usually found to increase with the size of the halogen[21].

In systems where both a halogen and hydrogen bond can be formed there may be competition between the two differing interactions. One of the current authors recently studied the competition of hydrogen and halogen

bonding interactions in complexes of 5-halogenated 1-methyluracil with one or two water molecules in the binding region between C4-X and C5=O6 (with X = F, Cl, Br, I or At)[22] see **Figure 1**, note in the previous paper we used a different atom numbering scheme C5-X ≡ C4-X and C4=O4 ≡ C5=O6. In the singly-hydrated systems, the water molecule was found to form a hydrogen bond with C5=O6 for all halogens; however, structures with a halogen bond between the water oxygen and C4-X were only found for X = Br, I and At.

In the current investigation we use QTAIM[23] as the theoretical framework to shed more light on hydrogen and halogen bond formation in 5-halogenated 1-methyl-uracil:H_2O systems, with the halogen X ={F, Cl, Br, I, At}. QTAIM is used to identify critical points in the total electronic charge density distribution $\rho(\mathbf{r})$ by analyzing $\nabla\rho(\mathbf{r})$. These critical points can further be divided into four types of topologically stable critical points according to the set of ordered eigenvalues $\lambda_1 < \lambda_2 < \lambda_3$, with corresponding eigenvectors $\underline{\mathbf{e}}_1$, $\underline{\mathbf{e}}_2$, $\underline{\mathbf{e}}_3$ of the Hessian matrix, i.e. the matrix of partial second derivatives of $\rho(\mathbf{r})$ with respect to the components of $\mathbf{r}$ evaluated at these points, using classifiers of the form (rank, signature), where the rank is the number of distinct eigenvalues and the signature is the sum of their numerical signs. These are denoted as: (3,-3), which are local maxima usually corresponding to a nuclear position (*NCP*), but can be non-nuclear maxima (*NNA*); other critical points are denoted as (3,-1) and (3,+1), which correspond to bond critical point (*BCP*) and ring critical point (*RCP*), respectively and are both saddle points; finally (3,+3) corresponds to cage critical point (*CCP*) which is a local minimum. The pair of special gradient paths linking a *BCP* with two nuclei (*NCP*s) and along which $\rho(\mathbf{r_b})$ is a maximum with respect to any neighboring path is denoted as an atomic interaction line (AIL)[24], where the subscript '$_b$' denotes the value at the *BCP*. In the limit that the forces on the nuclei become vanishingly small, an AIL becomes a bond-path, although not necessarily a chemical bond[25]. The complete set of critical points together with the bond-paths of a molecule or cluster is referred to as the molecular graph.

The ellipticity, ε provides the relative accumulation of $\rho(\mathbf{r_b})$ in the two directions perpendicular to the bond-path at a *BCP* and is defined as $\varepsilon = |\lambda_1|/|\lambda_2| - 1$, where λ_1 and λ_2 are negative eigenvalues of the corresponding Hessian matrix at the *BCP*[23]. A related quantity to the ellipticity ε for closed-shell interactions is the metallicity $\xi(\mathbf{r}_b)$[26,27] of a *BCP* defined as:

$$\xi(\mathbf{r}_b) = \rho(\mathbf{r}_b)/\nabla^2\rho(\mathbf{r}_b) \geq 1 \qquad \text{for} \qquad \nabla^2\rho(\mathbf{r}_b) > 0 \tag{1}$$

In recent work some of the current authors showed that the $\xi(\mathbf{r}_b)$ is inversely related to "nearsightedness" of the first-order density matrix and is suitable for closed-shell systems[28]. In this work we chose to assess the electron deficiency by using $\xi(\mathbf{r}_b)$ instead of σ-holes.

A *BCP* will possess shared-shell character before the bond-path is stretched sufficiently to transform the chemical character to closed-shell. As the bond-path is stretched the relative rate of decrease of the charge density $\rho(\mathbf{r}_b)$ compared with the Laplacian $\nabla^2\rho(\mathbf{r}_b)$ will be different resulting in a region of metallic character. The metallicity $\xi(\mathbf{r}_b)$ has been used previously to explore suspected metallicity ranges of metals, metalloids and non-metals[26,27]. From equation (1), closed-shell *BCP*s with a degree of metallicity, $\xi(\mathbf{r}_b) \geq 1$ often also possess a degree of covalent character, determined from the total local energy density $H(\mathbf{r}_b)$[29,30] that is defined as:

$$H(\mathbf{r}_b) = G(\mathbf{r}_b) + V(\mathbf{r}_b) \tag{2}$$

In equation **(2)**, $G(\mathbf{r}_b)$ and $V(\mathbf{r}_b)$ are the local kinetic and potential energy densities at a *BCP* respectively. A value of $H(\mathbf{r}_b) < 0$ for the closed-shell interaction, $\nabla^2\rho(\mathbf{r}_b) > 0$, indicates a *BCP* with a degree of covalent character, this can be acquired from an adjoining shared-shell *BCP*, that will increase the strength. Conversely $H(\mathbf{r}_b) > 0$ reveals a lack of covalent character for the closed-shell *BCP*. Previously[31,32], one of us found that the unusual strength of the (closed-shell) hydrogen bonds in ice Ih could be explained in terms the donation of covalent character from the (shared-shell) O-H sigma bond to the hydrogen bond in agreement with x-ray scattering experiment[33].

In this work the nomenclature A-B *BCP* refers to a shared-shell *BCP* to distinguish from the two classes of closed-shell *BCP*s; A--B *BCP* possesses a degree of covalent character with $H(\mathbf{r}_b) < 0$ and A---B *BCP* does not contain any covalent character possesses $H(\mathbf{r}_b) > 0$. We will not calculate bond energies or bond dissociation energies in this work either using topological atoms[34] or *BCP*s[35–37].

The 5X-1-methyluracil:H_2O energies were computed with the M06-2X functional[38] using the Gaussian 09 program[39]. Gaussian's "ultrafine" integration grid was employed. For systems incorporating F, Cl or Br the 6-31+G(d) basis set was employed, while for the systems containing I or At the aug-cc-p VDZ-PP basis set, which

includes small-core energy-consistent relativistic pseudo potentials (PP)[40], was employed to incorporate relativistic effects. Relaxed scans were created by varying the C4-X---O16(water) angle in steps of 1°, while all other geometrical parameters were freely optimized, see **Figure 1**. The QTAIM and stress analysis was performed with the AIMAll[41] suite on each wave function obtained along the IRC.

A schematic of the molecular graphs of the halogenated 1-methyluracil:H_2O systems indicating the O--H hydrogen-bond *BCP* connectivity as well as the X---O halogen-bond *BCP* connectivity, where X ={F, Cl, Br, I, At} are displayed in **Figure 1(a)**. For a sub-set, Y = {F, Cl, Br}, of the halogens the bond-path switches from the oxygen nucleus to the hydrogen nucleus, see **Figure 1(b)**. An example of bond-path switching; F18---O15 to F---H17 is given in **Figure 2(b)**. No bond-path switching behavior is associated with the hydrogen-bond *BCP*s of any of the halogenated 1-methyluracil:H_2O systems.


(a)   (b)

(c)   (d)   (e)
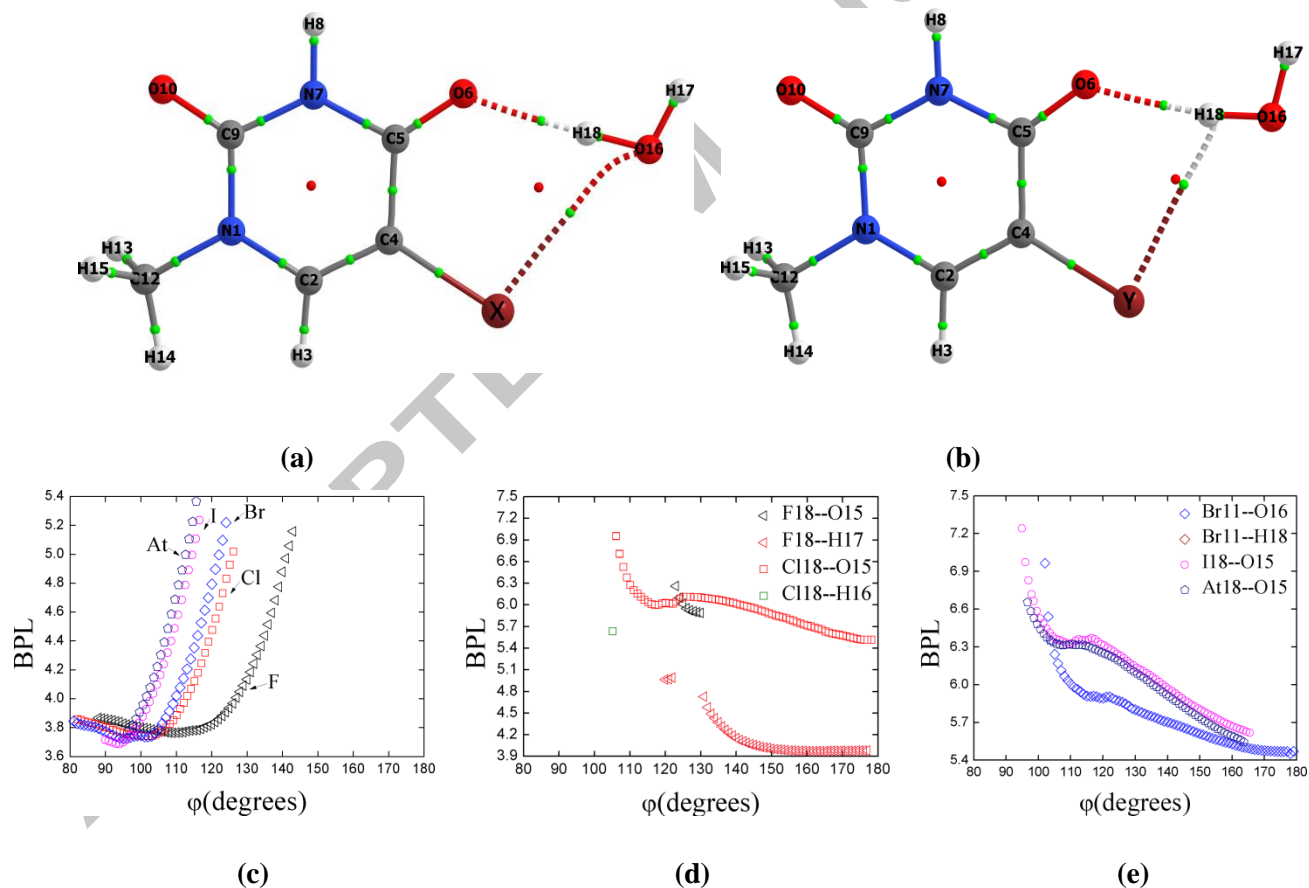
Figure 1. A schematic of a selection of the bonding topologies of the halogenated 1-methyluracil:H_2O molecular graphs, where X ={F, Cl, Br, I, At} and Y ={F, Cl, Br}, are presented in sub-figures **(a)** and **(b)** respectively. The undecorated green and red spheres represent the bond critical points (*BCP*s) and ring critical points (*RCP*s) respectively. The bond-path lengths (BPL) in a.u. of the hydrogen-bond *BCP*s and halogen-bond *BCP*s are shown in sub-figures **(c)** and **(d-e)** respectively. Note that the atom numbering scheme in sub-figure **(a-b)** differs from that used in the previous

investigation[22].

The hydrogen-bond *BCP* bond-path lengths (BPL) are considerably shorter than the corresponding X---O halogen-bond *BCP* bond-paths, see **Figure 1(c)** and **Figure 1(d-e)** respectively. The persistence of the hydrogen-bond *BCP*s with the reaction coordinate φ before the hydrogen-bond *BCP*s rupture decreases with the size of the halogen with F having the most persistent hydrogen-bond *BCP* with increase in the reaction coordinate φ. With the exception of the F---O *BCP* all of the halogen X---O *BCP*s persist for more of the reaction coordinate φ than do the hydrogen-bond *BCP*s indicating that the hydrogen-bond *BCP*s rupture more readily than the halogen bond *BCP*s. A simple relation however, between the persistence of the halogen X---O *BCP*s and halogen size, with the reaction coordinate φ is not found.
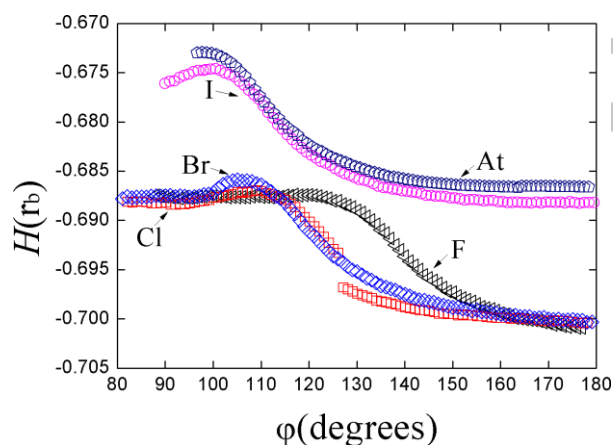
A negative value of the local energy density $H(\mathbf{r_b})$ for a closed-shell *BCP* indicates a degree of covalent character and is associated with cooperative polarization effects[29,30]. The hydrogen-bond *BCP*s and halogen-bond *BCP*s are indicated by circles and squares in **Figure 2,** respectively. It can be seen that the hydrogen-bond *BCP*s possess $H(\mathbf{r_b}) < 0$ only for Y = {F, Cl, Br}, with the degree of covalent character F > Cl > Br, see **Figure 2(a)**. The strength of the hydrogen-bond *BCP* in terms of $H(\mathbf{r_b}) < 0$ therefore was found to depend on the choice of X; this is in contrast to earlier work that found little dependence on the choice of X on the strength of the hydrogen bond[22].
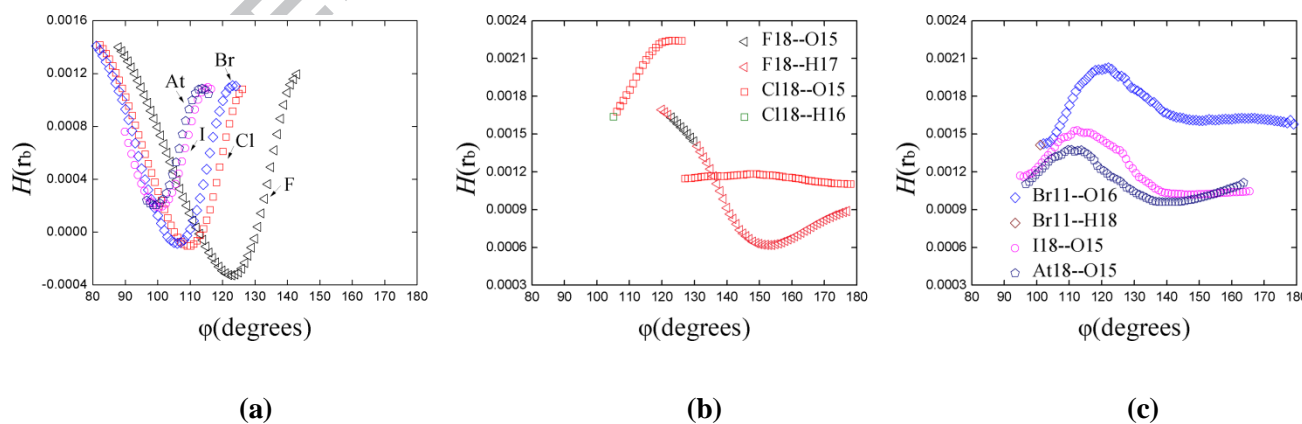
Figure 2. The variation of the total local energy density $H(\mathbf{r_b})$ in a.u. along the reaction coordinate φ for the halogen-bond *BCP* and hydrogen-bond *BCP* of the halogenated 1-methyluracil:H_2O molecular graphs.

All of the halogen-bond *BCP*s possess positive values of $H(\mathbf{r_b})$; therefore none possess any degree of covalent character and will be purely electrostatic in chemical character and therefore will not couple to the neighboring C4-X/C4--X *BCP*. The smooth switching of the bond-path associated with the F18---O15 *BCP* to that of the bond-path of the F18---H17 *BCP* $H(\mathbf{r_b})$ values is clearly evident, see **Figure 2(b)**. It can be noted that the F18---O15 *BCP* and associated bond-path only exists in the range of reaction coordinate φ, 123.0º ≤ φ ≤ 130.0º. The halogen-bond X---O *BCP* becomes more established along the reaction coordinate φ for X = Cl and Br, conversely the 'intermediate' Y---H *BCP* is less present along the reaction coordinate φ with increase in halogen size until I and At where there is no Y---H *BCP*.

If we consider the nearest neighbor of the hydrogen-bond *BCP*, that is the C5--O6 *BCP*, we find the unusual situation that the C5--O6 *BCP* has positive values of the Laplacian $\nabla^2\rho(\mathbf{r_b})$, i.e. a closed-shell *BCP*, and large negative values of the total local density $H(\mathbf{r_b})$, which would be expected from a shared-shell *BCP*, see **Figure 3**.

Figure 3. The variation of the total local energy density $H(\mathbf{r_b})$ in a.u. along the reaction coordinate φ for the C5--O6 *BCPs* of halogenated 1-methyluracil: H$_2$O molecular graphs. See the caption of **Figure 2** for further details.

It can be seen that the values of $H(\mathbf{r_b})$ of the C5--O6 *BCP* become less negative with increase in halogen size from F to At; this indicates a weakening of the C5--O6 closed-shell *BCP*. If we now consider the metallicity ξ(**r$_b$**) along the reaction coordinate φ for the C5--O6 *BCPs* we see that for the F, Cl and Br halogenated 1-methyluracil:H$_2$O there is considerably more metallicity ξ(**r$_b$**) than is present in the C5--O6 *BCPs* of the I and At halogenated 1-methyluracil:H$_2$O molecular graphs.
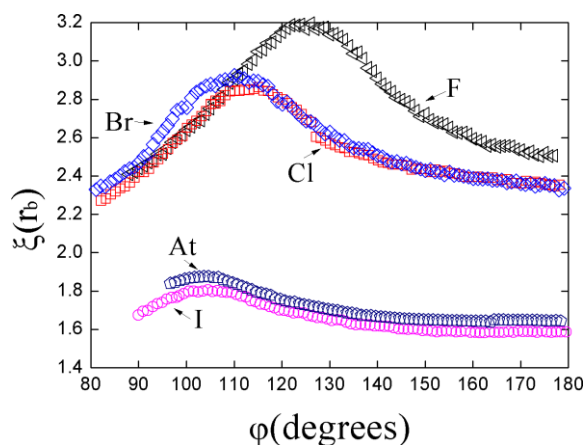
Figure 4. The variation of the metallicity $\xi(\mathbf{r}_b)$ along the reaction coordinate φ for the C5--O6 *BCPs* of halogenated 1-methyluracil:H_2O molecular graphs. See the caption of **Figure 2** for further details.

The lack of covalent character in the halogen X---O *BCPs* results in a lack of coupling with the nearest neighbor C4-X/C4--X *BCPs*. If coupling of the X---O *BCP* and C4-X/C4--X *BCPs* *were* present then the $H(\mathbf{r_b})$ values of the halogen X---O *BCPs* would be expected to reflect trends of the C4-X/C4--X *BCPs*. The $H(\mathbf{r_b})$ values the minima occur varies by almost an order of magnitude for the C4-X/C4--X *BCPs* in **Figure 5**. Conversely, the range of values of $H(\mathbf{r_b})$ of the hydrogen-bond *BCPs* is well within an order of magnitude, similar to that of the neighboring C5--O6 *BCPs*, due to the presence of coupling of the hydrogen-bond *BCPs* with the C5--O6 *BCPs*, see **Figure 2(a)** and **Figure 3**.
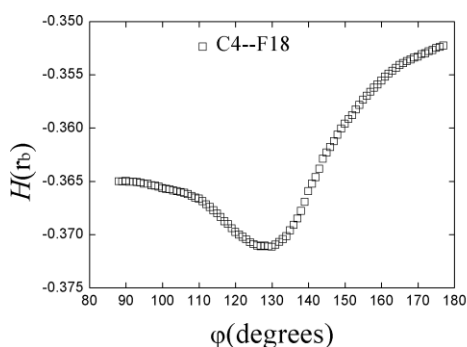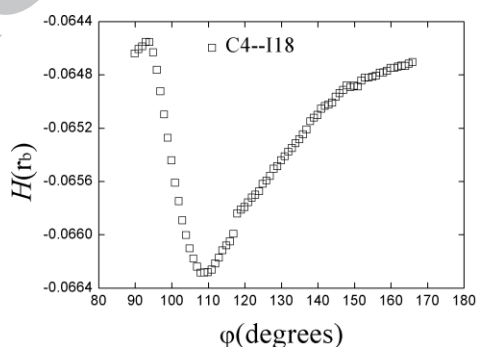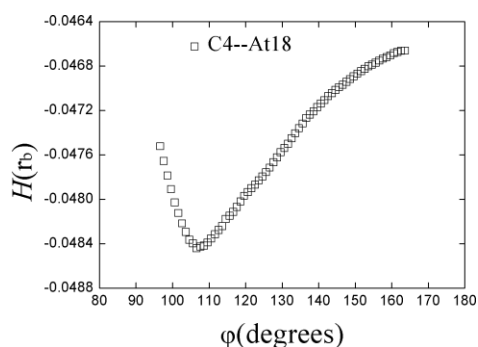

(a)
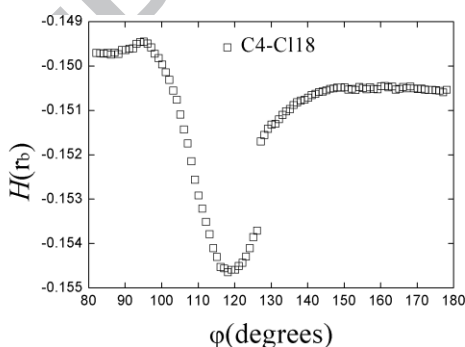
(b)
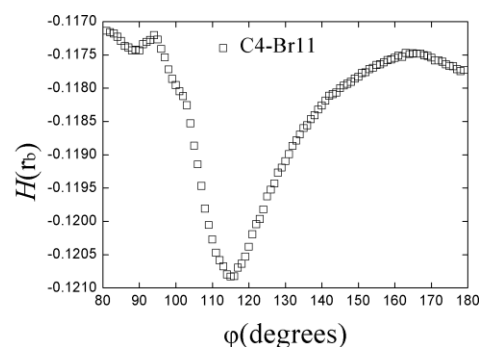
(c)

(d)

(e)

Figure 5. The variation of the total local energy density $H(\mathbf{r_b})$ in a.u. along the reaction coordinate φ for the C4-X/C4--X *BCPs* of halogenated 1-methyluracil: H_2O molecular graphs. See the caption of **Figure 2** for further details.

Significant metallicity $\xi(\mathbf{r_b})$, i.e. $\xi(\mathbf{r_b}) > 1$ for the C4--X *BCP* is only observed for the C4--I *BCP* and C4--At *BCP*, see **Figure 6**. We also notice the consequence of the absence of covalent character in the C4--X *BCP* in terms of the range of values and changing sign (-/+) of the $\xi(\mathbf{r_b})$ values of the C4-X/C4--X *BCPs*, e.g. $\xi(\mathbf{r_b}) < 0$ for the C4-C18 *BCP* and the C4-Br18 *BCP*, see **Figure 6(b-c)** but $\xi(\mathbf{r_b}) > 0$ for the remaining C4--X *BCPs* and **Figure 6(a)** and **Figure 6(d-e)**.

(a)   (b)   (c)

(d)   (e)
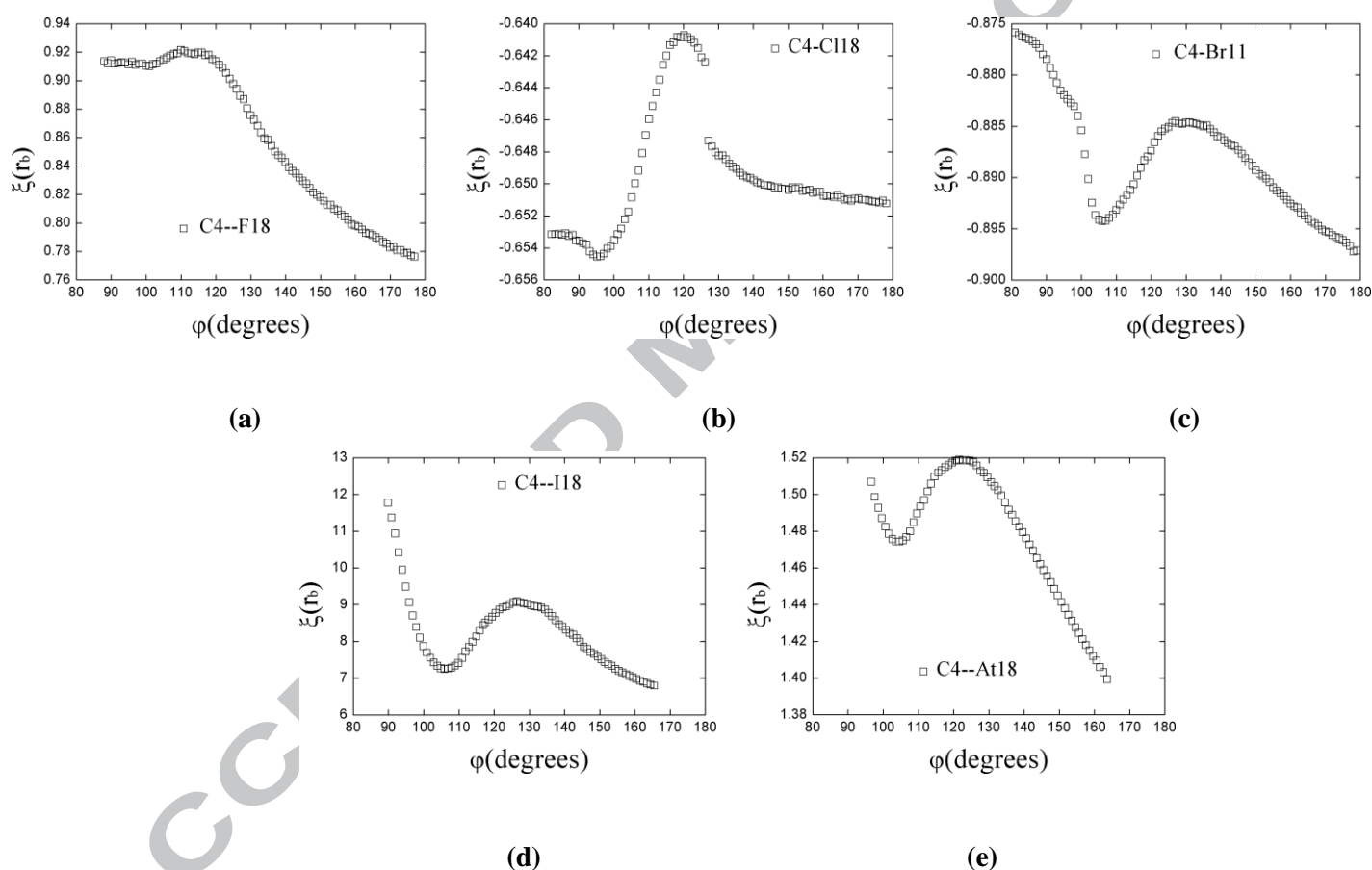
Figure 6. The variation of the metallicity $\xi(\mathbf{r_b})$ along the reaction coordinate φ for the C4--X *BCP* of halogenated 1-methyluracil: H_2O molecular graphs. See the caption of **Figure 2** for further details.

Using QTAIM to complement a previous energy-based approach[22], we investigated the hydrogen and halogen bonding in the region between the C4-X/C4--X *BCP* and the C5--O6 *BCP* and associated bond-paths in the 5-halogenated 1-methyluracil:H_2O molecular graphs with X = F, Cl, Br, I or At. For all X the water molecule was

found to form both hydrogen-bond *BCPs* and halogen-bond *BCP*s. The hydrogen-bond *BCP*s were found to be relatively stronger on the basis of negative values of $H(\mathbf{r_b})$ but ruptured more readily, since they exist for a smaller portion of the reaction coordinate φ, than the halogen-bond X---O *BCP*s with the exception of the F---O *BCP*, providing insights into the complexity of the competition between these bonding interactions.

The hydrogen-bond *BCP*s in the F-, Cl- and Br- containing halogenated molecular graphs were found to have mixed chemical character since $H(\mathbf{r_b}) < 0$, in contrast to the X---O halogen-bond *BCP*s that were all found to be purely electrostatic in character since $H(\mathbf{r_b}) > 0$. The hydrogen-bond *BCP*s in all cases were found to be stronger, on the basis of negative values of $H(\mathbf{r_b})$, than the halogen-bond *BCP*s. The additional strength of the hydrogen-bond *BCP*s can be explained by the presence of negative $H(\mathbf{r_b})$ values that enabled coupling with the neighboring C5--O6 *BCP*s that then 'donated' a degree of covalent character. The strength of the hydrogen-bond *BCP*s decreased with increase in size of the halogen. A weaker trend was found for the nearest neighbor C5--O6 *BCP* explainable in part by the lack of covalent character present for the hydrogen-bond *BCP*s with X = I and At. The halogen-bond X---O *BCP*s for X = Br, I and At strengthened with increase in halogen size. Conversely, the neighboring C4-X/C4--X *BCP* weakened with increase in halogen size, the lack of consistency between the X---O *BCP*s and the C4-X/C4--X *BCPs* can be explained by the lack of coupling due to the presence of positive $H(\mathbf{r_b})$ values for the X---O *BCP*s.

The controversial F---O halogen *BCP* only existed for a very small range of values, $123.0º \leq φ \leq 130.0º$ and away from the location minimum value at $φ \approx 150º$ in the total local energy density $H(\mathbf{r_b})$, providing an explanation as to why the F---O halogen bond was thought not to exist. The 'intermediate' F---H *BCP* and associated bond-path could be demonstrated to facilitate the creation of the F---O halogen-bond *BCP*. Intermediate Y---H *BCPs* were only found for Y = F, Cl and Br, although were only present to a significant extent for the F 5-halogenated 1-methyluracil:H_2O molecular graph. Only the F, Cl and Br halogenated molecular graphs contained stronger hydrogen-bond *BCP*s i.e. with a degree of covalent character, $H(\mathbf{r_b}) < 0$. The decrease in metallicity $\xi(\mathbf{r_b})$ of the hydrogen-bond *BCP* neighboring C5--O6 *BCP* with increase in halogen size could explain the lack of 'intermediate' Y---H *BCPs* for the heavier halogens; I and At.

Acknowledgements

References

1. Legon, A. C. The halogen bond: an interim perspective. *Phys. Chem. Chem. Phys.* **12,** 7736–7747 (2010).

2. Metrangolo, P., Neukirch, H., Pilati, T. & Resnati, G. Halogen Bonding Based Recognition Processes: A World Parallel to Hydrogen Bonding. *Acc. Chem. Res.* **38,** 386–395 (2005).

3. Politzer, P., Lane, P., Concha, M. C., Ma, Y. & Murray, J. S. An overview of halogen bonding. *J. Mol. Model.* **13,** 305–311 (2006).

4. Politzer, P., Murray, J. S. & Clark, T. Halogen bonding: an electrostatically-driven highly directional noncovalent interaction. *Phys. Chem. Chem. Phys.* **12,** 7748–7757 (2010).

5. Flurry, R. L. Molecular Orbital Theory of Electron Donor-Acceptor Complexes. I. A Simple Semiempirical Treatment. *J. Phys. Chem.* **69,** 1927–1933 (1965).

6. Aakeröy, C. B., Baldrighi, M., Desper, J., Metrangolo, P. & Resnati, G. Supramolecular Hierarchy among Halogen-Bond Donors. *Chem. – Eur. J.* **19,** 16240–16247 (2013).

7. Scheiner S, Kar T, Gu Y. Strength of the CαH•• O hydrogen bond of amino acid residues. *J. Biol. Chem.* **276,** 9832–9837 (2001).

8. Desiraju G R, Steiner T. Weak Hydrogen BondOxford University Press. *N. Y.* (1999).

9. Scholfield, M. R., Zanden, C. M. V., Carter, M. & Ho, P. S. Halogen bonding (X-bonding): A biological

    perspective. *Protein Sci.* **22,** 139–152 (2013).

10. Auffinger, P., Hays, F. A., Westhof, E. & Ho, P. S. Halogen bonds in biological molecules. *Proc. Natl.*

    Acad. Sci. U. S. A. **101,** 16789–16794 (2004).

11. Kawade, M. *et al.* Photodissociation Dynamics of Halogenated Thiophenes at 235 nm: A Resonance

    Enhanced Multiphoton Ionization-Time-of-Flight (REMPI-TOF) Study. *J. Phys. Chem. A* **116,** 10656–

    10667 (2012).

12. Riley, K. E., Ford Jr., C. L. & Demouchet, K. Comparison of hydrogen bonds, halogen bonds, CH··π

    interactions, and CX··π interactions using high-level ab initio methods. *Chem. Phys. Lett.* **621,** 165–170

    (2015).

13. Grant Hill, J. & Legon, A. C. On the directionality and non-linearity of halogen and hydrogen bonds. *Phys*

    Chem Chem Phys **17,** 858–867 (2015).

14. Riley, K. E. *et al.* Halogen bond tunability I: the effects of aromatic fluorine substitution on the strengths of

    halogen-bonding interactions involving chlorine, bromine, and iodine. *J. Mol. Model.* **17,** 3309–3318

    (2011).

15. Aakeröy, C. B., Fasulo, M., Schultheiss, N., Desper, J. & Moore, C. Structural Competition between

    Hydrogen Bonds and Halogen Bonds. *J. Am. Chem. Soc.* **129,** 13772–13773 (2007).

16. Riley, K. E. & Merz, K. M. Insights into the Strength and Origin of Halogen Bonding: The

    Halobenzene−Formaldehyde Dimer. *J. Phys. Chem. A* **111,** 1688–1694 (2007).

17. Riley, K. E. & Hobza, P. Investigations into the Nature of Halogen Bonding Including Symmetry Adapted Perturbation Theory Analyses. *J. Chem. Theory Comput.* **4,** 232–242 (2008).

18. Meazza, L. *et al.* Halogen-bonding-triggered supramolecular gel formation. *Nat. Chem.* **5,** 42–47 (2013).

19. Metrangolo, P., Meyer, F., Pilati, T., Resnati, G. & Terraneo, G. Halogenbrücken in der supramolekularen Chemie. *Angew. Chem.* **120,** 6206–6220 (2008).

20. Eskandari, K. & Lesani, M. Does Fluorine Participate in Halogen Bonding? *Chem. – Eur. J.* **21,** 4739–4746 (2015).

21. Priimagi, A. *et al.* Halogen Bonding versus Hydrogen Bonding in Driving Self-Assembly and Performance of Light-Responsive Supramolecular Polymers. *Adv. Funct. Mater.* **22,** 2572–2579 (2012).

22. Hogan, S. W. L. & van Mourik, T. Competition between hydrogen and halogen bonding in halogenated 1-methyluracil: Water systems. *J. Comput. Chem.* **37,** 763–770 (2016).

23. Bader, R. F. W. *Atoms in Molecules: A Quantum Theory*. (Oxford University Press, USA, 1994).

24. Bader, R. F. W. A Bond Path: A Universal Indicator of Bonded Interactions. *J. Phys. Chem. A* **102,** 7314–7323 (1998).

25. Bader, R. F. W. Bond Paths Are Not Chemical Bonds. *J. Phys. Chem. A* **113,** 10391–10396 (2009).

26. Jenkins, S. Direct space representation of metallicity and structural stability in SiO solids. *J. Phys. Condens. Matter* **14,** 10251–10263 (2002).

27. Jenkins, S., Ayers, P. W., Kirk, S. R., Mori-Sánchez, P. & Martín Pendás, A. Bond metallicity of materials from real space charge density distributions. *Chem. Phys. Lett.* **471,** 174–177 (2009).

28. Ayers, P. W. & Jenkins, S. Bond metallicity measures. *Comput. Theor. Chem.* **1053,** 112–122 (2015).

29. Cremer, D. & Kraka, E. Chemische Bindungen ohne Bindungselektronendichte -reicht die Differenzdichteanalyse zur Bindungsbeschreibung aus? *Angew. Chem.* **96,** 612–614 (1984).

30. Kraka, E. & Cremer, D. Description of chemical reactions in terms of the properties of the electron density. *J. Mol. Struct. THEOCHEM* **255,** 189–206 (1992).

31. Jenkins, S. & Morrison, I. The chemical character of the intermolecular bonds of seven phases of ice as revealed by ab initio calculation of electron densities. *Chem. Phys. Lett.* **317,** 97–102 (2000).

32. Jenkins, S., Restrepo, A., David, J., Yin, D. & Kirk, S. R. Spanning QTAIM topology phase diagrams of water isomers W4, W5 and W6. *Phys. Chem. Chem. Phys.* **13,** 11644–11656 (2011).

33. Isaacs, E. D. *et al.* Covalency of the Hydrogen Bond in Ice: A Direct X-Ray Measurement. *Phys. Rev. Lett.* **82,** 600–603 (1999).

34. Matta, C. F., Sadjadi, S. A., Braden, D. A. & Frenking, G. The barrier to the methyl rotation in Cis-2-butene and its isomerization energy to Trans-2-butene, revisited. *J. Comput. Chem.* **37,** 143–154 (2016).

35. Sadjadi, S., Matta, C. F. & Hamilton, I. P. Chemical bonding in groups 10, 11, and 12 transition metal homodimers — An electron density study. *Can. J. Chem.* **91,** 583–590 (2013).

36. SeyedAbdolreza Sadjadi†, Chérif F. Matta*‡§, Kono H. Lemke†, and I. P. Hamilton. Relativistic-Consistent Electron Densities of the Coinage Metal Clusters M2, M4, M42−, and M4Na2 (M = Cu, Ag, Au): A QTAIM Study. **115,** 13024–13035 (2011).

37. Espinosa, E., Molins, E. & Lecomte, C. Hydrogen bond strengths revealed by topological analyses of experimentally observed electron densities. *Chem. Phys. Lett.* **285,** 170–173 (1998).

38. Zhao, Y. & Truhlar, D. G. The M06 suite of density functionals for main group thermochemistry, thermochemical kinetics, noncovalent interactions, excited states, and transition elements: two new functionals and systematic testing of four M06-class functionals and 12 other functionals. *Theor. Chem. Acc. Theory Comput. Model.* **120,** 215–241 (2008).

39. Frisch, M. *et al. Gaussian 09, Revision B.01*. (Gaussian, Inc., 2009).

40. Peterson, K. A., Figgen, D., Goll, E., Stoll, H. & Dolg, M. Systematically convergent basis sets with relativistic pseudopotentials. II. Small-core pseudopotentials and correlation consistent basis sets for the post-d group 16–18 elements. *J. Chem. Phys.* **119,** 11113–11123 (2003).

41. Keith, T. A. *AIMAll*. (TK Gristmill Software, 2012).

- From QTAIM, hydrogen bonds were always found to be stronger than the corresponding halogen bonds in complexes of 5-halogenated-1-methyl-uracil:H_2O systems, X ={F, Cl, Br, I, At}.

- Hydrogen bonding displayed an admixture of covalent and purely electrostatic character.

- All halogen bonds were found to be purely electrostatic.

- The strength of the hydrogen bond decreased with increasing halogen size.

- An F---O halogen bond was found and was facilitated by an intermediate F---H bonding interaction.